Separation Science and Technology
Publication details, including instructions for authors and subscription information:
http://www.informaworld.com/smpp/title~content=t713708471

On Relaxation Phenomena in Field-Flow Fractionation

K. Jayaraj[a]; R. Shankar Subramanian[a]
[a] DEPARTMENT OF CHEMICAL ENGINEERING, CLARKSON COLLEGE OF TECHNOLOGY, NEW YORK

To cite this Article Jayaraj, K. and Subramanian, R. Shankar(1978) 'On Relaxation Phenomena in Field-Flow Fractionation', Separation Science and Technology, 13: 9, 791 — 817
To link to this Article: DOI: 10.1080/01496397808057128
URL: http://dx.doi.org/10.1080/01496397808057128

SEPARATION SCIENCE AND TECHNOLOGY, 13(9), pp. 791–817, 1978

On Relaxation Phenomena in Field-Flow Fractionation

K. JAYARAJ and R. SHANKAR SUBRAMANIAN*

DEPARTMENT OF CHEMICAL ENGINEERING
CLARKSON COLLEGE OF TECHNOLOGY
POTSDAM, NEW YORK 13676

Abstract

The two-dimensional unsteady convective diffusion equation satisfied by the local concentration of the colloid introduced in a field-flow fractionation (FFF) column is solved by the method of finite differences. The alternating direction implicit (ADI) method proposed by Peaceman and Rachford is used. The axial convection term is approximated by a backward difference approximation to obtain a stable and convergent scheme.

Numerical results are obtained for various values of the transverse Peclet number for the case of steady laminar flow and a slug input. The numerical results from the ADI method are validated by comparison with numerical solutions obtained using an explicit scheme as well as by internal consistency checks.

The results of this work show that the transverse concentration profiles depend in a complex fashion on axial position along the cloud during relaxation. In the presence of a field, asymptoticity in the transverse profiles is approached first in the rear of the colloid cloud, and progresses gradually through the axial extent of the cloud. Ultimately, at a sufficiently large value of time, almost all of the colloid relaxes to asymptotic exponential distributions in the transverse coordinate as predicted from theory. The local concentration of colloid in the system is observed to reach a global maximum value at intermediate values of time during relaxation. The area average concentration distribution is observed to exhibit strong asymmetry when plotted against the axial coordinate at intermediate times both in the presence and in the absence of a field. This asymmetry is in accord with pure convection theory. In contrast, truncated two-term dispersion equations only predict symmetric distributions for symmetric initial conditions. Thus there may be a need to retain higher order terms in the

*To whom all correspondence should be addressed.

application of generalized dispersion theory in order to predict the observed results.

INTRODUCTION

Field-flow fractionation (FFF) or polarization chromatography refers to a general class of methods used for the separation of colloidal mixtures. Described in several publications by Giddings and co-workers (*1–5*) and Lightfoot and co-workers (*6–8*), the technique involves the introduction of a colloid mixture at the inlet of a channel in which a suitable fluid is in laminar flow. As the various species move downstream, they are forced toward a system boundary either by transverse flow or by the use of suitable transverse fields. Ultimately, each colloidal solute relaxes to a unique asymptotic transverse distribution whose nature depends on the balance between its transverse migration and Brownian motion. In view of the nonuniform axial velocity field in the channel and the differences in the transverse concentration distributions among the colloids, the various species travel at different average velocities down the channel and may be separated.

Hovingh et al. (*8a*) have examined the relaxation of a colloid distribution in an FFF column using a pure convection model. More recently, Krishnamurthy and Subramanian (*9*) have developed a detailed theoretical description of the unsteady convective diffusion of a colloid in an FFF column right from time zero. These workers showed that the average concentration distribution of the colloid satisfies a generalized dispersion equation with time-variable coefficients. For practical reasons, they truncated their dispersion equation after two terms. It can be shown that such a truncated dispersion equation (TDE) will only predict average concentration distributions which are symmetric in the axial coordinate (about the center of gravity of the colloid) for initially symmetric colloid clouds. However, the experimental results of Yang et al. (*10*) suggest that axially asymmetric colloid distributions may exist in an FFF column during the relaxation period. It is quite possible that the initial distributions in the above experiments were not symmetric in the axial coordinate which may very well explain the shape of the reported breakthrough curves. But it is interesting and important to determine if, indeed, an independent solution of the governing equations would predict asymmetries for an initially symmetric distribution. Also, during the initial stages of the relaxation process, solute accumulates near a system boundary, resulting in large local concentrations at that boundary. At larger

values of time, concentrations generally decrease because of the axial spreading of the colloidal solute. Therefore, a global maximum of the local concentration may be reached during the relaxation period. Such a maximum is of considerable interest since large values of colloid concentration would make the assumption of a dilute system less realistic in theoretical analyses.* For this reason, and for developing a better physical understanding of the relaxation process during which most of the axial spreading of the colloid occurs in a typical high-field-strength application of FFF, it is important to examine local concentration distributions of the colloid during relaxation. In principle, it is possible to use analytical solutions such as those of Tseng and Besant (*11*) or DeGance and Johns (*12*) for calculating local concentration profiles. Also, truncated versions of generalized dispersion theory may be used for such calculations. However, the labor involved is substantial, and in the present work a numerical solution of the governing equations has been obtained using the method of finite differences in view of the relative simplicity of this technique. It is found that the numerical results of this work are physically realistic and provide a lot of useful information regarding the convective diffusion process in an FFF column.

ANALYSIS

The unsteady convective diffusion of a colloid introduced into a FFF column will be analyzed. The column is assumed to be made of two parallel plates w units apart and b units wide. The coordinate system is shown in Fig. 1. The primary flow is in the z-direction with a velocity

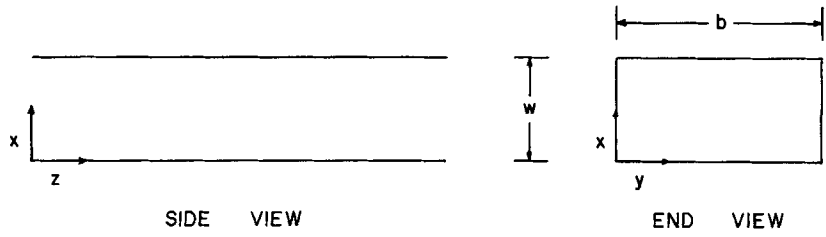

FIG. 1. The coordinate system.

*In concentrated systems, the effects of particle–particle and/or particle–wall interactions may be quite complex. For instance, Myers et al. (*28*) observed decreasing retention as they increased the particle concentration in the injected sample in FFF experiments. Such a result is likely to be caused by such interactions.

field $u(x)$, and a transverse field applied across the channel causes the migration of the colloid in the negative x-direction with a constant velocity v. Assuming the system to be dilute (and ignoring free convection effects), and further assuming a large aspect ratio ($b/w \gg 1$), the convective diffusion equation describing the local concentration of colloid may be written as

$$\frac{\partial c}{\partial t} + u(x)\frac{\partial c}{\partial z} - v\frac{\partial c}{\partial x} = D\left(\frac{\partial^2 c}{\partial x^2} + \frac{\partial^2 c}{\partial z^2}\right) \tag{1}$$

For simplicity, the present calculations are restricted to the following initial condition:

$$\left.\begin{aligned} c(0, x, z) &= c_0, \qquad |z| \leq \frac{1}{2}z_s \\ &= 0, \qquad |z| > \frac{1}{2}z_s \end{aligned}\right\} \tag{2a}$$

This initial condition describes a slug of colloid of uniform concentration c_0. The slug is uniform in the transverse coordinate x, and is z_s units long. It is located symmetrically about $z = 0$. Since the walls of the column are impermeable to the colloid, assuming no adsorption of the colloid on these walls, the flux of the colloid across either wall is zero. Therefore,

$$-D\frac{\partial c}{\partial x}(t, 0, z) - vc(t, 0, z) = 0 \tag{2b}$$

$$-D\frac{\partial c}{\partial x}(t, w, z) - vc(t, w, z) = 0 \tag{2c}$$

Since the amount of colloid introduced is finite,

$$c(t, x, \pm\infty) = 0 \tag{2d}$$

The axial velocity field is given by

$$u(x) = 6u_m\left(\frac{x}{w} - \frac{x^2}{w^2}\right) \tag{2e}$$

Using the dimensionless variables and parameters defined in the section on "Symbols," Eqs. (1) and (2) may be rewritten in dimensionless form as

$$\frac{\partial C}{\partial T} + U(X)\frac{\partial C}{\partial Z} - \mathrm{Pe}_t\frac{\partial C}{\partial X} = \frac{\partial^2 C}{\partial X^2} + \frac{1}{\mathrm{Pe}^2}\frac{\partial^2 C}{\partial Z^2} \tag{3}$$

$$\left.\begin{aligned} C(0, X, Z) &= 1, \qquad |Z| \leq \frac{1}{2}Z_s \\ &= 0, \qquad |Z| > \frac{1}{2}Z_s \end{aligned}\right\} \tag{4a}$$

$$\frac{\partial C}{\partial X}(T, 0, Z) = -\mathrm{Pe}_t C(T, 0, Z) \tag{4b}$$

$$\frac{\partial C}{\partial X}(T, 1, Z) = -\mathrm{Pe}_t C(T, 1, Z) \tag{4c}$$

$$C(T, X, \pm\infty) = 0 \tag{4d}$$

$$U(X) = 6(X - X^2) \tag{4e}$$

Equations (3) and (4) were solved in the present work using finite difference techniques [Jayaraj (*13*)].* The alternating direction implicit (ADI) technique proposed by Peaceman and Rachford (*14*) and discussed by Douglas (*15*) was employed for the solution. When convection dominates diffusion, as is the case in the axial direction in the present problem, conventional central difference approximations of the convection term result in unstable schemes. For instance, instabilities were observed by Gill and Ananthakrishnan (*16*) in their ADI solution of convective diffusion in a capillary. To overcome this problem, Runchal and Wolfshtein (*17*) proposed the use of a backward (with respect to the flow) difference approximation of the convection term. This upwind difference scheme (UDS) is unconditionally stable and quite accurate when sufficiently small space intervals are employed. Spalding (*18*) and Runchal (*19*) later suggested another modification of UDS which is stable and accurate at all values of the (axial) Peclet number, Pe. This procedure reduces to the central difference scheme at low Peclet numbers and to UDS at high Peclet numbers. Since under typical operating conditions the axial Peclet number Pe is large in an FFF column, a value of Pe = 1000 was chosen for use in the present calculations. For this value

*The grid points in Z were equally spaced initially, with the spacing being increased at larger times to handle the increased axial extent of the colloid. The grid spacing in the transverse coordinate X was nonuniform for nonzero Pe_t—the smallest spacing was at $X = 0$ with the spacing increasing in geometric progression for increasing X. This grid-point distribution was selected over the simple equal-size grids because of the exponential nature of the asymptotic transverse distributions, and proved to be convenient.

of Pe, the UDS is quite acceptable, and therefore it was used in calculating all the results reported here. Since it is not possible to account for boundaries at infinity in a numerical scheme, axial stations sufficiently far away from the colloid distribution were chosen as artificial axial boundaries on the system. These boundaries were moved farther out as necessary during the course of the calculations. The results of the numerical calculations using the ADI method were checked in several ways for consistency and accuracy. These included comparisons with numerical results from explicit schemes and tests for convergence using smaller interval sizes. Also, the first axial moments of the area and bulk average concentrations from finite difference results may be used to calculate the coefficients $K_1(T)$ and $K_2(T)$ of generalized dispersion theory. These were checked against the results of Krishnamurthy and Subramanian (*9*) after suitable conversion of the dimensionless variables. Generally, the agreement was excellent at $Pe_t = 0$ and was still quite good at the largest Pe_t ($Pe_t = 30$) investigated in this work [the deviations in $K_2(T)$ varied from 0.5% for $Pe_t = 0$ to 3.5% for $Pe_t = 30$, with typical deviations being under 1%; the deviations in $K_1(T)$ were much smaller]. A detailed discussion of the accuracy of the numerical solutions reported here may be found in Jayaraj (*13*). It should be emphasized that $K_1(T)$ and $K_2(T)$ were computed from the axial moments of the numerical solution strictly for the purpose of validating the numerical solution. Since a complete knowledge of the local concentration field immediately implies a complete knowledge of the average concentration field, the finite difference procedure is not an acceptable alternative to dispersion theories for the purpose of predicting dispersion coefficients—the theories permit the calculation of such coefficients from first principles without ever having to compute either the local or the average concentration field.

Since it is desired to compare the results of the present work for the area average concentration of the colloid with the solution of the truncated dispersion equation (TDE) of Krishnamurthy and Subramanian (*9*), their TDE in the present notation is given below:

$$\frac{\partial C_m}{\partial T} = K_1(T)\frac{\partial C_m}{\partial Z} + K_2(T)\frac{\partial^2 C_m}{\partial Z^2} \tag{5}$$

Here $C_m(T, Z)$ is the area average concentration defined by

$$C_m(T, Z) = \int_0^1 C(T, X, Z)\, dX \tag{6}$$

The initial condition on $C_m(T, Z)$ is obtained from Eqs. (4a) and (6) as

$$\left.\begin{aligned} C_m(0, Z) &= 1, \qquad |Z| \leq \frac{1}{2}Z_s \\ &= 0, \qquad |Z| > \frac{1}{2}Z_s \end{aligned}\right\} \tag{7}$$

The boundary conditions on C_m are obtained from Eq. (4d) as

$$C_m(T, \pm\infty) = 0 \tag{8}$$

The solution of Eqs. (7) and (8) is well-known [see, for instance, Gill and Sankarasubramanian (*20*)]:

$$C_m(T, Z) = \frac{1}{2}\left[\operatorname{erf}\left(\frac{\frac{1}{2}Z_s - Z_1}{2\sqrt{\xi}}\right) + \operatorname{erf}\left(\frac{\frac{1}{2}Z_s + Z_1}{2\sqrt{\xi}}\right)\right] \tag{9}$$

Here

$$Z_1 = Z + \eta(T) \tag{10a}$$

$$\eta(T) = \int_0^T K_1(\gamma)\, d\gamma \tag{10b}$$

and

$$\xi(T) = \int_0^T K_2(\gamma)\, d\gamma \tag{10c}$$

Results from Eq. (9) for $C_m(T, Z)$ will be referred to as the solution of the "truncated dispersion equation" in the present discussions. The results were evaluated using the computer programs developed by Krishnamurthy (*21*) after suitable conversion of dimensionless variables. The correspondence between the dimensionless variables used in the present numerical work and those used by Krishnamurthy and Subramanian (*9*) is summarized by Jayaraj (*13*).

In the limit of $\mathrm{Pe}_t = 0$ (no field), the pure convection solution (which ignores diffusion) may be expected to describe system behavior at least in a qualitative sense for small values of time. For $\mathrm{Pe}_t = 0$, ignoring diffusion, Eq. (3) reduces to

$$\frac{\partial C}{\partial T} + U(X)\frac{\partial C}{\partial Z} = 0 \tag{11}$$

The initial condition on C_m is given in Eq. (4a). The solution of the

equations obtained using the method of characteristics is given below:

$$\left.\begin{aligned} C(T, X, Z) &= 1, \quad |Z - U(X)T| \le \tfrac{1}{2}Z_s \\ &= 0, \quad |Z - U(X)T| > \tfrac{1}{2}Z_s \end{aligned}\right\} \tag{12}$$

From Eqs. (6) and (12), the cross-sectional average concentration $C_m(T, Z)$ under pure convection conditions is given by the following results:

For $T \le \frac{2}{3}Z_s$,

$$C_m = 0, \quad Z \le -\frac{1}{2}Z_s \tag{13a}$$

$$= 1 - \sqrt{1 - \frac{(Z + \frac{1}{2}Z_s)}{1.5T}}, \quad \left(-\frac{1}{2}Z_s < Z \le 1.5T - \frac{1}{2}Z_s\right) \tag{13b}$$

$$= 1, \quad \left(1.5T - \frac{1}{2}Z_s < Z < \frac{1}{2}Z_s\right) \tag{13c}$$

$$= \sqrt{1 - \frac{(Z - \frac{1}{2}Z_s)}{1.5T}}, \quad \left(\frac{1}{2}Z_s < Z < 1.5T + \frac{1}{2}Z_s\right) \tag{13d}$$

$$= 0, \quad \left(Z > 1.5T + \frac{1}{2}Z_s\right) \tag{13e}$$

For $T > \frac{2}{3}Z_s$,

$$C_m = 0, \quad Z \le -\frac{1}{2}Z_s \tag{14a}$$

$$= 1 - \sqrt{1 - \frac{(Z + \frac{1}{2}Z_s)}{1.5T}}, \quad \left(-\frac{1}{2}Z_s < Z \le \frac{1}{2}Z_s\right) \tag{14b}$$

$$= \sqrt{1 - \frac{(Z - \frac{1}{2}Z_s)}{1.5T}} - \sqrt{1 - \frac{(Z + \frac{1}{2}Z_s)}{1.5T}}, \quad \left(\frac{1}{2}Z_s < Z \le 1.5T - \frac{1}{2}Z_s\right) \tag{14c}$$

$$= \sqrt{1 - \frac{(Z - \frac{1}{2}Z_s)}{1.5T}}, \quad \left(1.5T - \frac{1}{2}Z_s < Z \le 1.5T + \frac{1}{2}Z_s\right) \tag{14d}$$

$$= 0, \quad \left(Z > 1.5T + \frac{1}{2}Z_s\right) \tag{14e}$$

When $Pe_t \neq 0$, the calculation of the pure convection solution is slightly more complex. This is because colloid retention at the lower boundary ($X = 0$) will have to be accounted for in an artificial manner in the solution. For the purposes of the present work, Eqs. (13) and (14) for the case of $Pe_t = 0$ are adequate.

RESULTS AND DISCUSSION

The ADI method was used in this work to calculate the dimensionless local concentration C as a function of dimensionless time T, the dimensionless transverse coordinate X, and the dimensionless axial coordinate Z. In addition to its dependence on T, X, and Z, C also depends parametrically on the axial Peclet number Pe, the transverse Peclet number Pe_t (equal to twice the parameter P used by Krishnamurthy and Subramanian), and the dimensionless slug length, Z_s. All the computations were performed for Pe = 1000 which is a typical value for a FFF column. Values of $Pe_t = 0$, 5, 10, and 30 were investigated systematically. In all the cases, different slug lengths in the range 0.01 to 0.1 were examined. The results judged to be most interesting will be presented here. More details may be found in Jayaraj (*13*). For convenience in the subsequent discussion, the results are divided into two cases—$Pe_t = 0$ and $Pe_t \neq 0$. The former corresponds to the case of no transverse field.

Special Case of No Field ($Pe_t = 0$)

This case was studied as a logical first step before attempting the more complex case of $Pe_t \neq 0$. Even though the analogous problem in a circular tube has been investigated numerically by Ananthakrishnan and Gill (*16*) and Bailey and Gogarty (*22*), finite difference solutions for the parallel-plate geometry have not been reported in the literature. Analytical results from generalized dispersion theory are available in Hsieh (*23*).* The numerical results for $Pe_t = 0$ are useful as a comparison standard for the $Pe_t \neq 0$ case, and also are sufficiently interesting and new that they are discussed in some detail here. Local concentration distributions can be effectively displayed in the form of isopleths of constant concentration. Figure 2 shows isopleths at a dimensionless time $T = 0.025$. The figure clearly shows the expected symmetry of

*For $Pe_t = 0$, $K_1(T) = -1$ for all values of time for a uniform initial distribution. It was convenient to evaluate $\xi(T)$ using Krishnamurthy's (*21*) computer programs which calculated Hsieh's results in the limit $Pe_t = 0$.

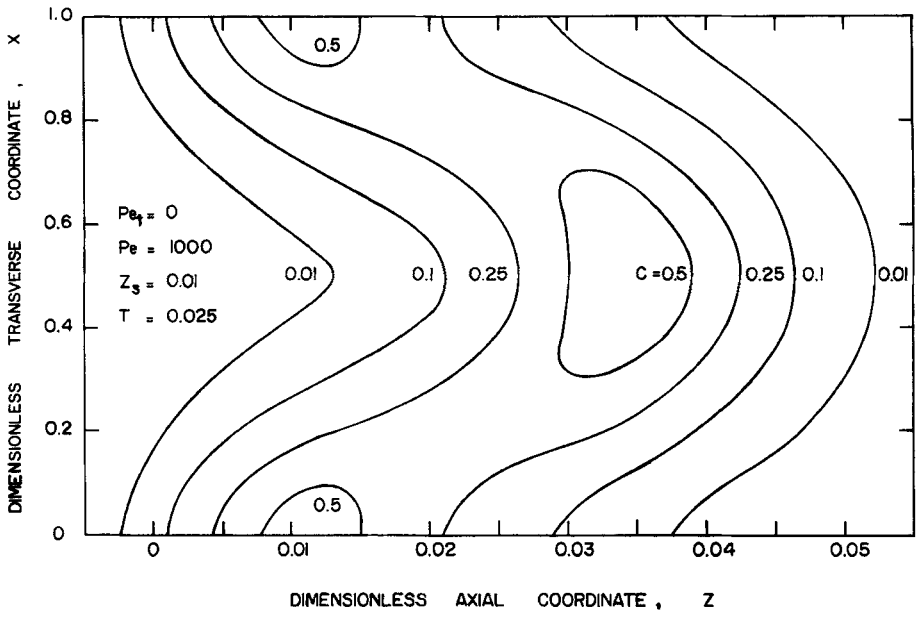

FIG. 2. Isopleths of constant concentration as functions of dimensionless transverse and axial coordinates.

these curves about the centerline ($X = 0.5$). There appear to be zones of high concentration near the center of the channel and close to the channel walls in the (axially) central regions of the distribution. This can be explained as follows. At the center, the velocity gradients are negligible and axial dispersion of the solute originally present at the center can be expected to be minimal. Near the walls, the velocity gradients are large but the actual velocities are quite small, and hence the axial dispersion of the solute is relatively small. From these curves one may expect the area average concentration distribution in the axial coordinate to have a sharp front and a long tail similar to a pure convection model.

Figure 3 shows a comparison of area-average concentration distributions at $T = 0.025$ from the present calculations with results from the two-term truncated dispersion theory and the pure convection model. The dimensionless area average concentration C_m is plotted as a function of the dimensionless axial coordinate Z in the figure. The figure shows the pure convection solution to be highly asymmetric in the axial coordinate. This is the case for a parallel plate channel when the center of the rear end of

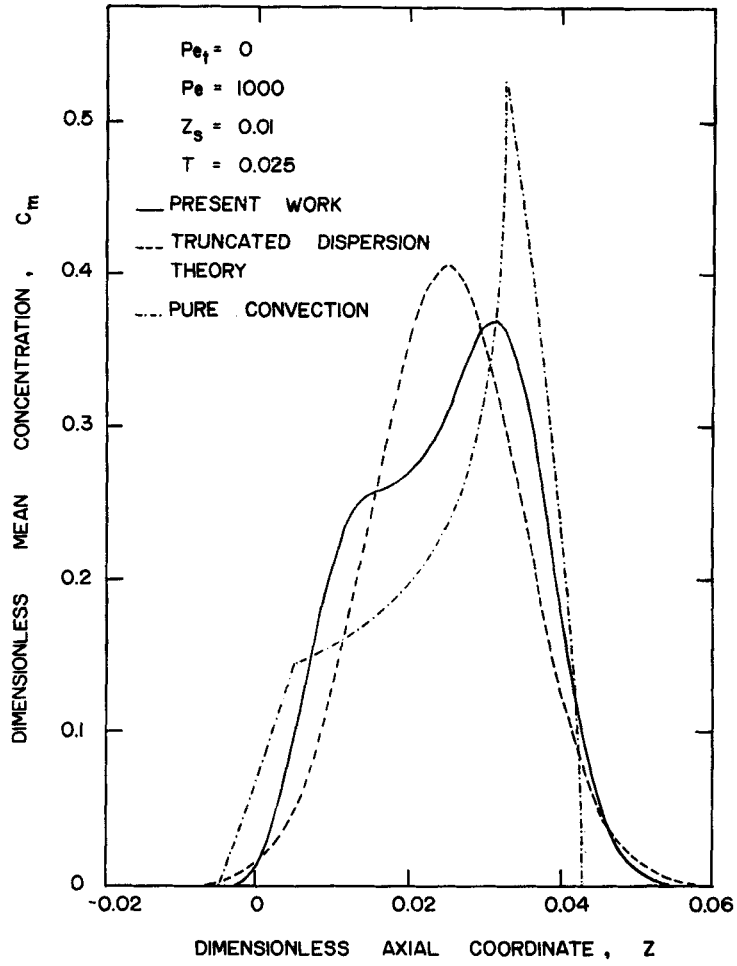

FIG. 3. Comparison of dimensionless mean concentration against dimensionless axial coordinate from the present work, from Krishnamurthy and Subramanian (*9*), and from the pure convection solution.

the slug moving at the maximum velocity of flow has moved past the axial station occupied by the front end of the initial slug ($T \geq 0.667Z_s$). The change of slope in the C_m vs Z plot occurs at $Z = \frac{1}{2}Z_s$. *Concentration distributions for the purely convective dispersion of a slug in a circular capillary under similar conditions are always symmetric about their center of gravity.* This is the reason why the limitations of the two-term dispersion equation (which only predicts symmetric profiles in Z for symmetric initial conditions) did not become apparent earlier. The figure shows the numerical solution to be in qualitative agreement with the pure convection solution while being more realistic in smoothing out the sharp corners in the latter solution. Furthermore, the changes in slope as well as the peak are seen to occur very close to the locations predicted by the pure convection model, thus promoting confidence in the numerical solution. From the figure it is clear that higher order terms need to be retained in the generalized dispersion equation to predict the observed behavior of the area-average concentration accurately. However, it should be pointed out that the ith truncated version of generalized dispersion theory predicts the first $(i + 1)$ axial moments (both power moments and Hermite moments) of the solute distribution precisely. For instance, by suitable integration of the generalized dispersion equation, Subramanian (*24*) shows how the temporal integrals of the coefficients $K_i(T)$ of generalized dispersion theory are related to the corresponding power moments of the solute distribution. DeGance and Johns (*12*), in an elegant development of the theory of dispersion problems, show that the i'th dispersion approximation predicts the first $(i + 1)$ Hermite moments precisely. They further speculate that such an approximation may even excite the higher order Hermite moments in the proper direction. An examination of the pure convection solutions reported in Eqs. (13) and (14) reveals that a knee in the distribution corresponding to a rapid change of slope at $Z = \frac{1}{2}Z_s$ predicted by Eqs. (14b) and (14c) materializes only when $T \geqslant \frac{2}{3}Z_s$. This was indeed observed to be the case in the present numerical work. Furthermore, from intuition, one may expect the knee in the profiles to be smoothed out at large values of time due to the persistent action of diffusion. To a first approximation, the diffusion time across the channel half-width may be estimated to be on the order of $T \sim 0.125$. This would mean that a knee in the average concentration profiles may be observed only in the time range $0.667Z_s \lesssim T \lesssim 0.125$. Therefore, for a sufficiently long slug ($0.667Z_s \gtrsim 0.125$), the knee should never materialize. It appears that the above estimate is conservative since no knee was observed even when calculations were made for a slug of dimensionless length $Z_s = 0.1$ (not reported here).

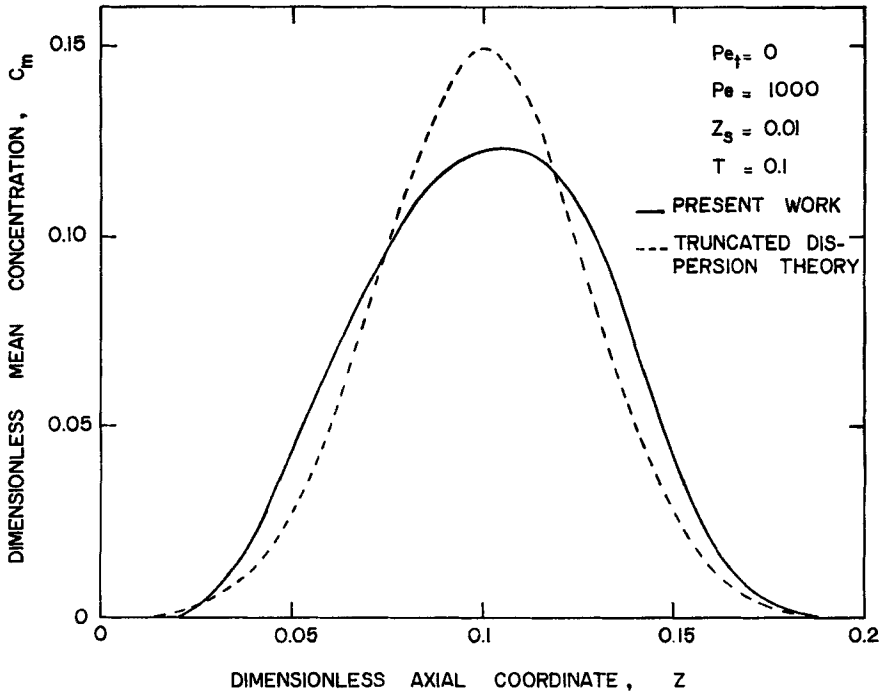

FIG. 4. Comparison of dimensionless mean concentration against dimensionless axial coordinate from the present work and from Krishnamurthy and Subramanian (*9*).

Figure 4 shows the dimensionless average concentration distribution as a function of the dimensionless axial coordinate at $T = 0.1$, a value of time sufficiently large for the knee to be smoothed out. However, considerable differences still exist between the solution of the two-term dispersion equation and the finite difference results. Small differences still persist at larger times even though they may become less important as time increases. The accuracy of the finite difference calculations would become progressively worse at larger times due to accumulating errors. Hence the differences seen in Fig. 4 and in results at larger T values may possibly be due to such errors. However, the possibility cannot be ruled out that higher order dispersion approximations may bring the analytical results closer to those of the numerical work.

It is interesting to see how well the two-term dispersion approximation predicts transverse concentration distributions. In generalized

dispersion theory, $C(T, X, Z)$ is given by

$$C(T, X, Z) \sim \sum_{k=0}^{\infty} f_k(T, X) \frac{\partial^k C_m}{\partial Z^k} \tag{15}$$

where the functions $f_k(T, X)$ are obtained from first principles. For a transversely uniform initial distribution with $\mathrm{Pe}_t = 0$,

$$f_0 \equiv 1 \tag{16}$$

Use of Eq. (16) in (15), and slight rearrangement, lead to

$$C - C_m \sim \sum_{k=1}^{\infty} f_k(T, X) \frac{\partial^k C_m}{\partial Z^k} \tag{17}$$

Equation (17) suggests that transverse concentration profiles will, in general, depend on axial position. However, a first approximation to the right-hand side gives

$$\frac{C - C_m}{\dfrac{\partial C_m}{\partial Z}} \sim f_1(T, X) \text{ only} \tag{18}$$

Since a similar approximation is involved in the derivation of the two-term dispersion equation (Eq. 5), it is interesting to check if the predictions of Eq. (18) are reasonable at any value of time. Plots at three different axial locations of the left-hand side in Eq. (18) calculated from the numerical results are shown in Fig. 5 for a small value of time, $T = 0.025$. The figure also shows the function $f_1(T, X)$ at this value of time, calculated from dispersion theory (Hsieh's results were converted to the present system of dimensionless variables for presentation). It may be seen from the figure that, at this value of time, the truncation of the solution of generalized dispersion theory implied in Eq. (18) leads to unrealistic predictions of local concentration behavior in the central region of the distribution while being qualitatively correct in the front and rear regions of the same slug. This is understandable since $\partial C_m/\partial Z$ is very small in the central region whereas the next higher derivative is not. The figure points to the need to include more terms in the right-hand side of Eq. (18) for the proper description of local concentration distributions at small values of time. It was found that at larger values of T ($T \gtrsim 0.5$), the left-hand side of Eq. (18) reaches asymptoticity in the transverse coordinate and is independent of Z over most of the solute cloud. Agreement with

$$f_{1\infty}(X) = \lim_{T \to \infty} f_1(T, X)$$

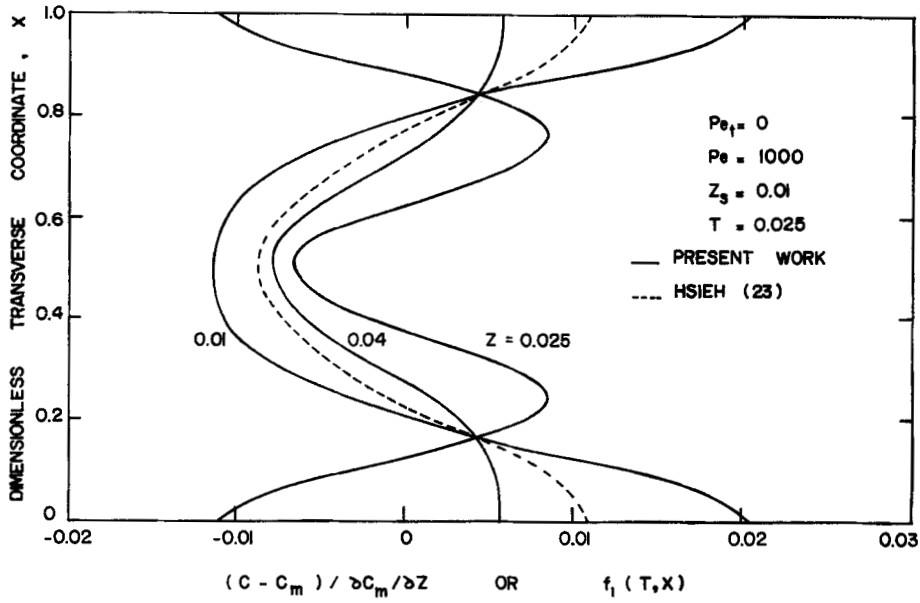

FIG. 5. Comparison of $(C - C_m)/(\partial C_m/\partial Z)$ against dimensionless transverse coordinate from the present work at $Z = 0.01$, 0.025, and 0.04 with $f_1(T, X)$ from Hsieh (*23*).

from Hsieh (*23*) was very good. Thus Eq. (18) is a viable result for sufficiently large values of time. Figure 6 shows the isopleths at $T = 0.5$ which demonstrate the extent of transverse mixing achieved by diffusion at such large values of time. The small values of C reflect the dilution due to axial spreading.

Nonzero Pe_t

The relaxation of an initially uniform colloid slug is described by Figs. 7 to 10 for $Pe_t = 5$, which is a typical value for a FFF column. Figure 7 shows the isopleths at a relatively small value of the dimensionless time ($T = 0.025$). From the figure it may be observed that the colloid has generally begun to accumulate near the lower wall of the channel, while the region near the upper wall is correspondingly depleted of colloid. The isopleths in the central region are not too different from those in the case of no field. This is to be expected for such small values of time when the central region of flow simply receives material from above

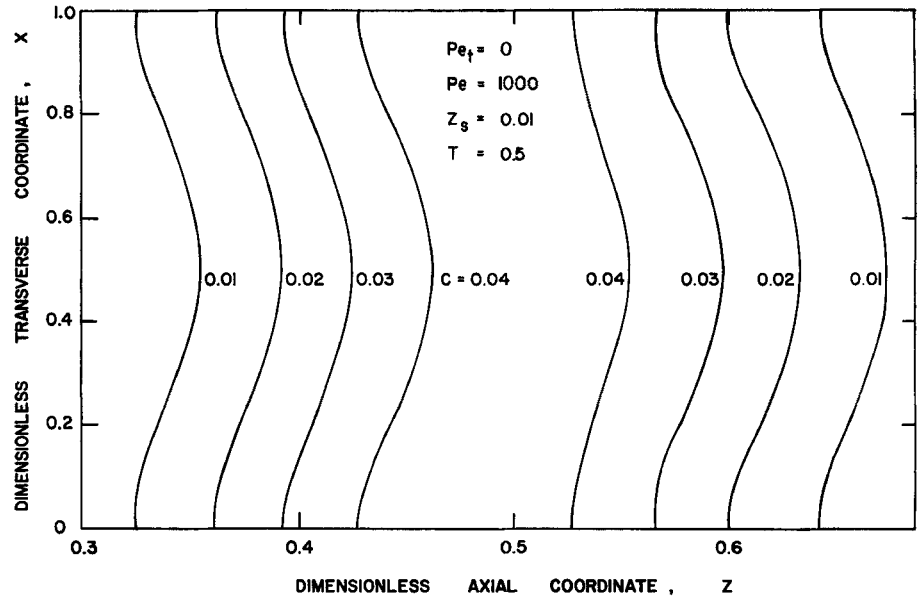

FIG. 6. Isopleths of constant concentration as functions of dimensionless transverse and axial coordinates.

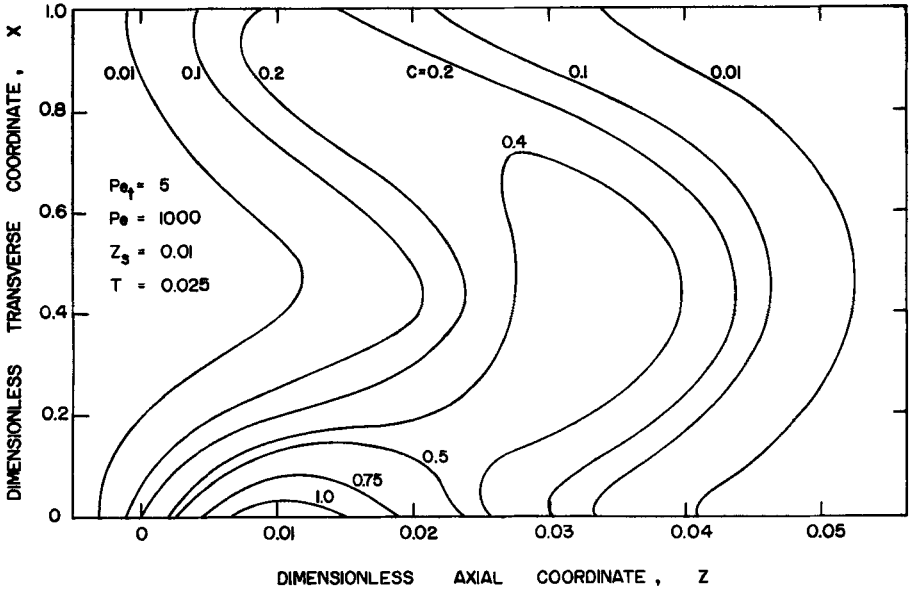

FIG. 7. Isopleths of constant concentration as functions of dimensionless transverse and axial coordinates.

(due to the action of the field) and transmits it to the regions below. The one difference is that the pocket of high concentration observed at the center in the case of no field seems to have moved down and merged with the similar pocket observed at the wall. The transverse gradients in the rear end of the colloid distribution are much sharper than those at the front. Also, at the rear, the transverse distribution has begun to approach asymptoticity. It is clear from Fig. 7 that the colloid concentration distribution at this value of time is a complex function of both transverse and axial position. Furthermore, the actual transverse distributions appear to vary widely over the axial extent of the colloid. These distributions are plotted at selected axial locations in Fig. 8 for the same set of parameters used in Fig. 7. $Z = 0.005$ corresponds to an axial location near the rear end of the distribution. It may be seen that colloid has been convected away from the central region of the channel (near $X = 0.5$) while there is colloid accumulation near the bottom wall. Near the upper boundary, with slower moving fluid, colloid still is present

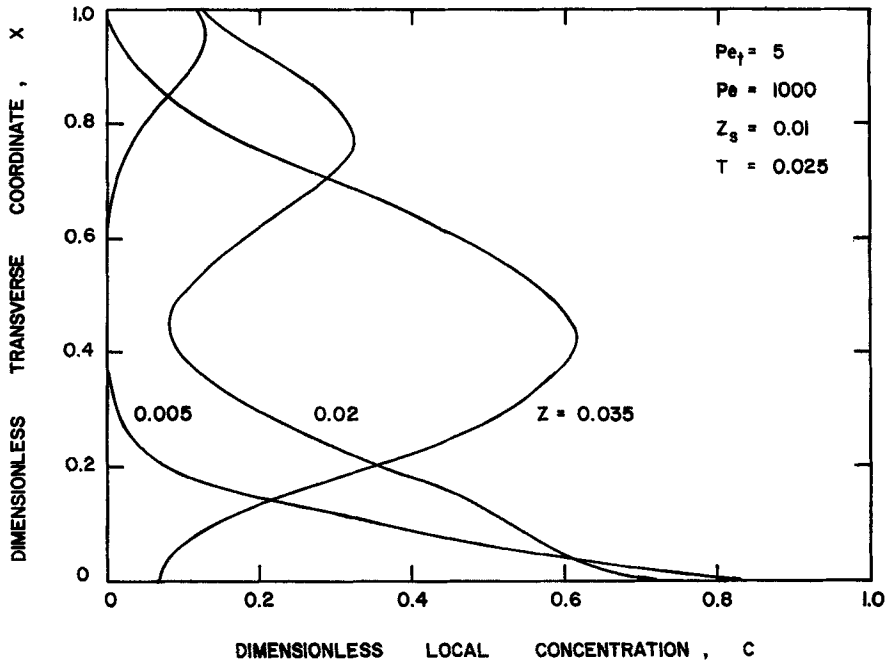

FIG. 8. Plots of dimensionless local concentration against dimensionless transverse coordinate at $Z = 0.005$, 0.02, and 0.035.

in significant quantities. Similar behavior is observed at $Z = 0.02$, a location near the center of the axial extent of the colloid. However, in the rear end of the colloid distribution (at $Z = 0.005$), steeper transverse concentration gradients may be observed near the lower boundary. In fact, at this axial station the distribution looks very similar to the asymptote anticipated over the entire axial extent of the colloid at large time. The rear end is quick to reach the asymptotic condition since no new colloid deposition near the lower boundary will occur at larger values of time. From a physical point of view, it may be expected that the asymptotic transverse distributions reflecting a balance between transverse migration and diffusion will be reached first near the rear end and will progressively occur at larger values of time over the axial extent of the colloid. This was indeed observed during the course of the present calculations. For completeness, the transverse concentration profile near the front end of the colloid distribution ($Z = 0.035$) also is plotted in Fig. 8. The similarity of system behavior at such axial stations to the no-field case is evident from the figure.

Figure 9 shows isopleths for $\mathrm{Pe}_t = 5$ at a relatively large value of the dimensionless time ($T = 0.5$). At this time, as may be seen from the figure, the relaxation process appears to be near completion over almost the entire axial extent of the colloid cloud. The nearly parallel isopleths indicate similarity in the transverse concentration profiles. One can also expect the concentrations to be symmetric with respect to a properly chosen axial location. The similarity of the transverse concentration profiles is demonstrated by Fig. 10. The transverse distributions at three axial locations are plotted using the wall concentration as the scale factor for each location. $Z = 0.25$, 0.35, and 0.5 correspond to axial locations in the rear, center, and front regions of the distribution, respectively. In the generalized dispersion theory of Krishnamurthy and Subramanian (*9*), the local concentration $C(T, X, Z)$ is written in the form given in Eq. (11). However, even when the initial distribution is uniform in X, because of the presence of the field, $f_0(T, X) \neq 1$, and instead, asymptotically approaches an exponential function of X. Therefore, when the derivatives $\partial^k C_m/\partial Z^k$ ($k = 1, 2, 3, \ldots$) are small, Eq. (15) may be approximated by

$$C \sim f_0(T, X) C_m(T, Z) \tag{19}$$

Equation (19) predicts that the shapes of transverse concentration profiles would be similar at all axial locations, and would be given by $f_0(T, X)$. Figure 8 shows that this is not true at small values of T, and higher order

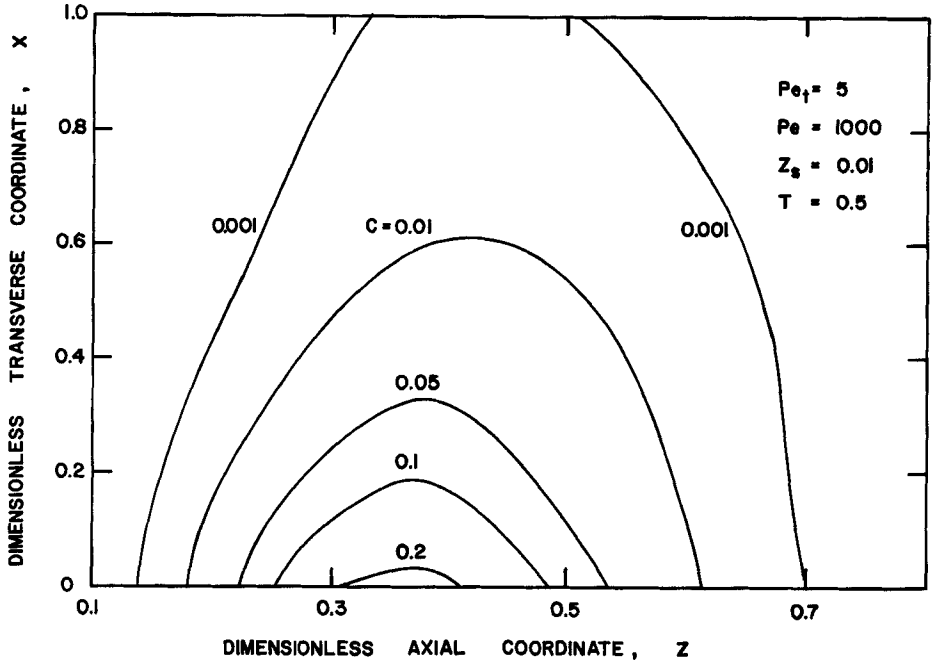

FIG. 9. Isopleths of constant concentration as functions of dimensionless transverse and axial coordinates.

terms would need to be included in the right-hand side of Eq. (19). However, at large T, Eq. (19) is a good approximation, as shown by the similarity of the transverse concentration profiles in Fig. 10. Plotted for comparison purposes in the same figure is $f_0(T, X)$ with $f_0(T, 0)$ used as a scale factor. At $T = 0.5$, $f_0(T, X)$ is practically independent of T and is given by Krishnamurthy and Subramanian as

$$f_0(T, X) \simeq f_{0s}(X) = f_{0s}(0)e^{-Pe_t X} \tag{20}$$

The agreement in Fig. 10 among the various profiles is quite satisfactory. The figure shows better agreement of $f_0(T, X)$ with the transverse concentration profile near the center of the colloid cloud than with the other two profiles. This is to be expected since $\partial C_m/\partial Z$ is very small near the center of the distribution, and Eq. (19) is practically a second-order approximation. It also is of interest to note here that the exponential transverse concentration distributions observed in Fig. 10 at large times

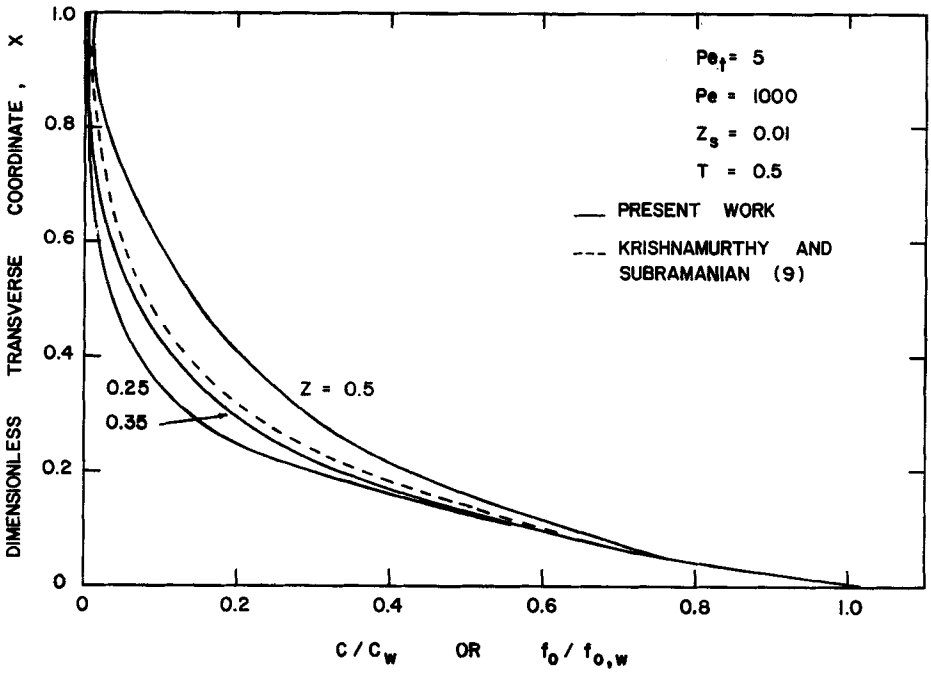

FIG. 10. Plots of dimensionless local concentration against dimensionless transverse coordinate from the present work and $f_0(T, X)$ against the dimensionless transverse coordinate from Krishnamurthy and Subramanian (*9*) (all scaled using the values at the wall).

were predicted by Giddings (*25*) who presented an asymptotic theory of FFF using intuitive assumptions similar to those of Taylor (*26*).

For purposes of comparison, Fig. 11 shows the isopleths at $T = 0.05$ for a large value of the transverse Peclet number ($Pe_t = 30$). It is seen from the figure that this relatively small value of time is adequate for the colloid distribution to reach a relaxed asymptotic state. From the predictions of Krishnamurthy and Subramanian, relaxation may be expected to occur in this system for $T \lesssim 1/Pe_t$. It should be noted that the ordinate is marked from 0 to 0.3 in this figure. Therefore, the transverse extent of the colloid is very narrow, as one would expect. Very high concentrations are observed in regions close to the lower boundary, and practically all the solute is contained in the region $X \gtrsim 0.25$. It was observed by Jayaraj (*13*) that the transverse distributions at different axial stations are all similar and merge into one profile when the wall

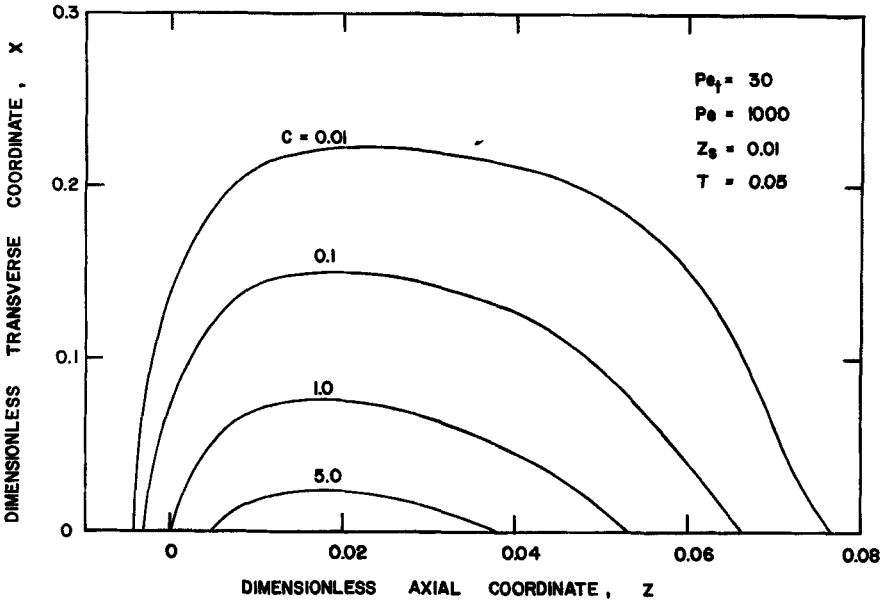

FIG. 11. Isopleths of constant concentration as functions of dimensionless transverse and axial coordinates.

concentration is used as a scale factor, in agreement with theory. The profile also is indistinguishable from $f_0(T, X)$ scaled by $f_0(T, 0)$.

Maximum Concentrations

The values of the maximum colloid concentrations reached in the system are of considerable interest since a large concentration buildup will lead to particle–particle interactions, osmotic effects, etc., and may ultimately limit the strength of the field that may be employed. As the colloid begins its journey through an FFF column, colloid buildup occurs initially at the lower wall, leading to large concentrations. However, this process cannot continue indefinitely because of the diluting effect of the axial dispersion of the colloid caused by velocity gradients. Ultimately, as time approaches infinity, the colloid concentration must approach zero everywhere. Therefore, the concentration must peak out at some intermediate value of time during relaxation. The present finite difference results permit the determination of the maximum concentrations and the times at which they occur for various transverse Peclet numbers. It was

observed that over most of the axial extent of the distribution, the maximum concentrations occurred at the lower wall ($X = 0$), as expected. At $Pe_t = 5$, the maximum concentration at $T = 0.005$ was observed at $Z = 0.004$, slightly behind the center of the distribution. However, the location of the maximum concentration in this case moved axially at a considerably lower velocity than the average velocity of the colloid, and the maximum concentration was found to occur consistently in the rear end of the colloid cloud. For $Pe_t = 5$, a global maximum local concentration equal to approximately twice the initial concentration in the colloid slug was observed at $T \approx 0.01$ and $Z \approx 0.005$. In contrast, for $Pe_t = 30$, the global maximum local concentration reached was approximately 11 times the initial concentration and occurred at $T \approx 0.02$ and $Z \approx 0.007$. In both cases, C_{max} was reached during the relaxation period, and could not have been computed from any other solution technique known at this time. The large C_{max} value for $Pe_t = 30$ indicates that the assumption of a dilute system used in the analyses of FFF columns may not be a good one.

Figures 12 and 13 show a comparison of the average concentration distributions computed using the finite difference method with the solution of the truncated two-term dispersion equation (TDE) from the generalized dispersion theory of Krishnamurthy and Subramanian (*9*). The figures are plotted for one typical value of the transverse Peclet number ($Pe_t = 10$). However, the distributions remained qualitatively similar at the other values of Pe_t investigated in this work ($Pe_t = 1, 5, 10, 20, 30$). Figure 12 shows the comparison at a value of dimensionless time $T = 0.025$. The TDE predicts a symmetric axial concentration distribution whereas the numerical results show a knee in the concentration profile—similar differences were seen in the limit of no field, $Pe_t = 0$. Figure 13, plotted at $T = 0.5$, shows the knee in the finite difference results has been smoothed out, but minor differences still persist between the two solutions. Interestingly, it is seen that the finite difference peak which was ahead of the two-term dispersion theory peak in Fig. 12 has now moved behind the dispersion theory peak. This is because of the relatively large amount of colloid contained in the rear half of the colloid cloud at the smaller value of time in Fig. 12. As the knee is smoothed out by convective diffusion, this excess material results in the lagging of the finite difference peak behind the TDE peak.

The results for the average concentration distributions for $Pe_t \neq 0$ are qualitatively similar to those reported for the limit of no field ($Pe_t = 0$) and indicate that higher order terms may be important enough to include

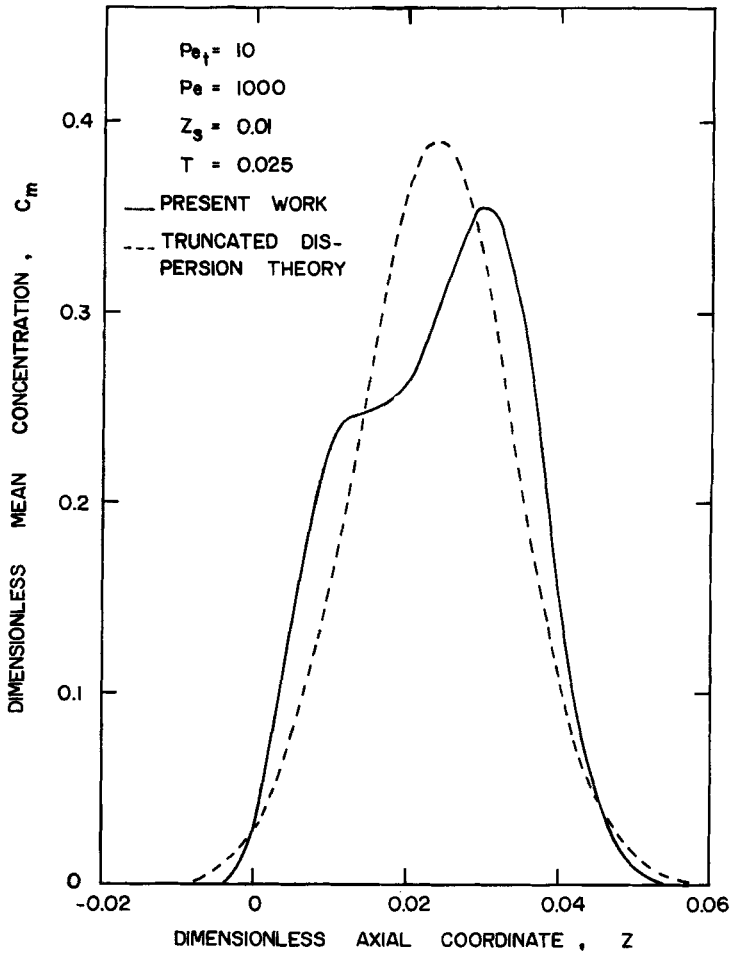

FIG. 12. Comparison of dimensionless mean concentration against dimensionless axial coordinate from the present work and from Krishnamurthy and Subramanian (*9*).

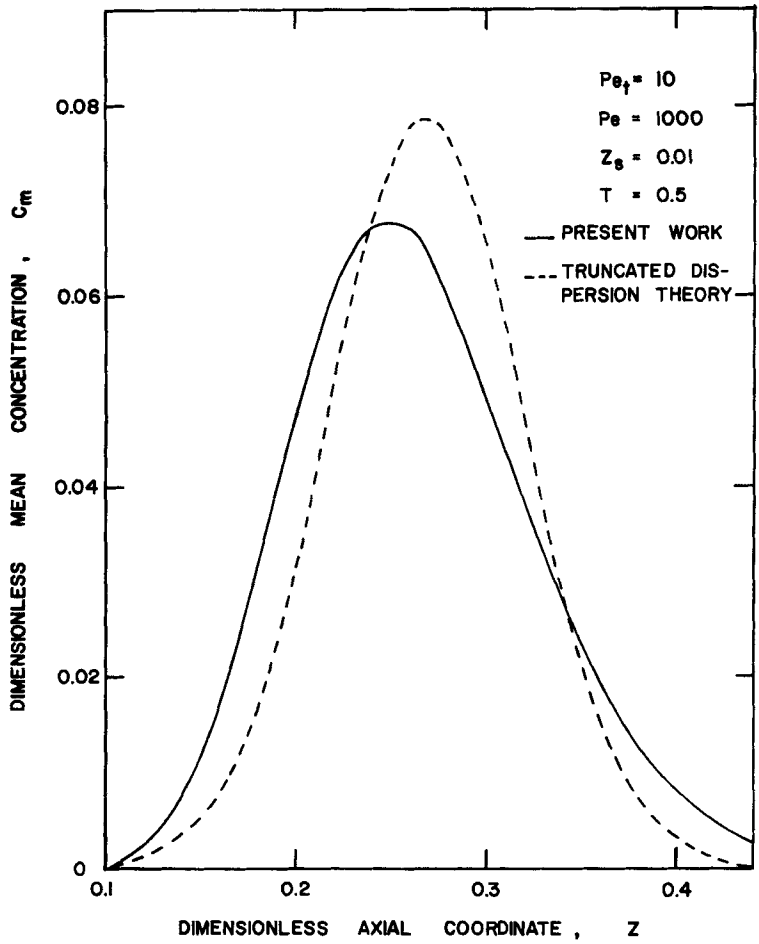

FIG. 13. Comparison of dimensionless mean concentration against the dimensionless axial coordinate from the present work and from Krishnamurthy and Subramanian (*9*).

in truncated dispersion equations. The resulting higher order partial differential equations may perhaps be solved using techniques such as those of Gola et al. (*27*).

CONCLUSIONS

The unsteady transport of a colloid introduced in a FFF column has been analyzed. An unconditionally stable ADI method was used to solve the convective diffusion equation numerically, and the results have been verified using an explicit scheme at small values of time. Results from the present work show a complex dependence of transverse concentration profiles on the axial coordinate during relaxation. Asymptoticity of these profiles is observed first in the rear region of the colloid cloud and progressively propagates through the entire axial extent. Comparisons with results from dispersion theory show that the function f_0 of Krishnamurthy and Subramanian (*9*) is a good first-order approximation for the transverse profiles in a FFF column at sufficiently large values of time.

It has been shown that the largest values of the local concentration in a FFF column occur during the relaxation period. The present numerical results indicate that the assumption of a dilute system may have to be relaxed for large values of the transverse Peclet number.

The convection and dispersion coefficients calculated from the present work show good agreement with the results of Krishnamurthy and Subramanian, thus promoting confidence in both results. However, axial average concentration distributions exhibit strong asymmetry at intermediate values of time in accordance with pure convection theory. These results are in disagreement with the predictions of a truncated two-term dispersion theory, thus pointing to a need to include higher order terms in the analytical results.

SYMBOLS

b	channel width in the y-direction
C	dimensionless concentration; c/c_0
C_m	area average concentration defined in Eq. (6)
c	local concentration of colloid
c_0	reference concentration: initial concentration in the slug
D	molecular diffusivity of colloid
f_k	coefficient functions in Eq. (15)

f_{0s} steady-state asymptote of f_0
K_i coefficients in generalized dispersion equation
Pe axial Peclet number, $\text{Pe} = u_m w/D$
Pe_t transverse Peclet number, $\text{Pe}_t = vw/D$
T dimensionless time; $T = Dt/w^2$
t time
U dimensionless axial velocity; $U = u/u_m$
u axial velocity
u_m reference velocity: average axial velocity
v transverse migration velocity
w channel spacing in the x-direction
X dimensionless transverse coordinate; $X = x/w$
x transverse coordinate shown in Fig. 1
y lateral coordinate shown in Fig. 1
Z dimensionless axial coordinate; $Z = z/w\text{Pe}$
Z_s dimensionless slug length; $Z_s = z_s/w\text{Pe}$
z axial coordinate shown in Fig. 1
z_s slug length

Acknowledgments

Acknowledgment is made to the donors of the Petroleum Research Fund administered by the American Chemical Society for providing partial support for this research through PRF Grant 8363-G5. Also, this work was supported in part by the National Science Foundation through NSF Grant ENG76-06863.

REFERENCES

1. J. C. Giddings, *Sep. Sci.*, *1*, 123 (1966).
2. G. H. Thompson, M. N. Myers, and J. C. Giddings, *Anal. Chem.*, *41*(10), 1219 (1969).
3. L. F. Kesner, K. D. Caldwell, M. N. Myers, and J. C. Giddings, *Ibid.*, *48*(13), 1834 (1976).
4. J. C. Giddings, F. J. F. Yang, and M. N. Myers, *Ibid.*, *46*(13), 1917 (1976).
5. J. C. Giddings, F. J. F. Yang, and M. N. Myers, *Science*, *193*, 1244 (1976).
6. H. L. Lee, J. F. G. Reis, J. Dohner, and E. N. Lightfoot, *AIChE J.*, *20*(4), 776 (1974).
7. H. L. Lee and E. N. Lightfoot, *Sep. Sci.*, *11*(5), 417 (1976).
8. J. F. G. Reis and E. N. Lightfoot, *AIChE J.*, *22*(4), 779 (1976).
8a. M. E. Hovingh, G. H. Thompson, and J. C. Giddings, *Anal. Chem.*, *42*(2), 195 (1970).
9. S. Krishnamurthy and R. S. Subramanian, *Sep. Sci.*, *12*(4), 347 (1977).

10. F. J. Yang, M. N. Myers, and J. C. Giddings, *Anal. Chem.*, *49*(4), 659 (1977).
11. C. M. Tseng and R. W. Besant, *Proc. R. Soc. London*, *A317*, 91 (1970).
12. A. E. DeGance and L. E. Johns, "The Theory of Dispersion of Chemically Active Solute in a Rectilinear Flow Field," *Appl. Sci. Res.*, In Press.
13. K. Jayaraj, "Relaxation Phenomena in Field Flow Fractionation," M.S. Thesis, Clarkson College of Technology, 1977.
14. D. W. Peaceman and H. H. Rachford, Jr., *J. Soc. Ind. Appl. Math.*, *3*(1), 28 (1955).
15. J. Douglas, Jr., *Ibid.*, *3*(1), 42 (1955).
16. W. N. Gill and V. Ananthakrishnan, *AIChE J.*, *13*(4), 801 (1967).
17. A. K. Runchal and M. Wolfshtein, *J. Mech. Eng. Sci.*, *11*(5), 445 (1969).
18. D. B. Spalding, *Int. J. Num. Meth. Eng.*, *4*, 551 (1972).
19. A. K. Runchal, *Ibid.*, *4*, 541 (1972).
20. W. N. Gill and R. Sankarasubramanian, *Proc. R. Soc. London*, *A316*, 341 (1970).
21. S. Krishnamurthy, "Exact Analysis of Field Flow Fractionation," M.S. Thesis, Clarkson College of Technology, 1976.
22. H. R. Bailey and W. B. Gogarty, *Proc. R. Soc. London*, *A269*, 352 (1962).
23. H. Hsieh, "Dispersion in Open Channel Laminar Flows," M.S. Thesis, Clarkson College of Technology, 1971.
24. R. S. Subramanian, *J. Chromatogr.*, *101*, 253 (1974).
25. J. C. Giddings, *J. Chem. Phys.*, *49*(1), 81 (1968).
26. G. I. Taylor, *Proc. R. Soc. London*, *A219*, 186 (1953).
27. E. Gola, A. Marani, F. Avezzu, R. Dabala, and A. Paratella, *Ing. Chim.* (*Ital.*), *9*, 89 (1973).
28. M. N. Myers, K. D. Caldwell, and J. C. Giddings, *Sep. Sci.*, *9*(1), 47 (1974).

Received by editor April 3, 1978